

# In-situ production of WC-Ni using a laser cladding technique

Samuel Skhosane<sup>1</sup>, Bathusile Masina<sup>1,2</sup>, Paul Lekoadi<sup>1</sup> & Sisa Pityane<sup>1,3</sup>

<sup>1</sup>Manufacturing Cluster, Photonics Center, Council for Scientific and Industrial Research, South Africa

<sup>2</sup>Department of Mechanical Engineering Science, University of Johannesburg, South Africa

<sup>3</sup>Department of Chemical and Metallurgical Engineering, Tshwane University of Technology, South Africa

**Abstract.** Metal Matrix Composite (MMC) coatings of Tungsten Carbide (WC) and Nickel (Ni) powder were produced using laser cladding process. A crack free and good metallurgically bonded WC-Ni coating of about 5mm thick produced from varying both laser energy density and percent mixture of Ni and WC. In this study, the microstructure of WC-Ni coatings were characterised using optical microscope (OM), scanning electron microscope (SEM) with EDS, while mechanical properties of the coating were studied using Vickers hardness tester and abrasion wear resistance tester. It was found that the hardness and wear resistance increase as the percentage of WC increases.

## 1 Introduction

Component that are used in abrasive mechanical environment they often need to pose high hardness, good wear resistance and corrosion resistance [1]. Mining industry is rated as an extremely abrasive environment which requires good wear resistance material such as tungsten carbide (WC), niobium carbide (NbC) etc [2]. Mining industry uses Ground engineering tools (GETs) for digging mineral ore, however, these GETs suffers from abrasive wear during digging and loading of ore [2]. Poor life span of GETs reduces the production rate while increase down time and maintenance cost.

Improving the life span of this GETs, one would look at improving wear resistance since most mining tool failed due to wear. Most research in mining sector focus on studying how to improve this mining GETs [3, 4]. Hard-facing these GETs with hard material might bring solution to the life span of these GETs, material such as NbC and WC are amongst the material that are most focused on to be used as hard-facing. WC is mostly known of its superior wear resistance and durability material within the engineering sector and mining sector [3], it is one of the metal-matrix composites(MMC) that has success in fabrication of cutting tool and drill bits inserts in mining industry [4]. This hard composite has high temperature wear resistance, low thermal expansion, good corrosion resistance, flexural strength, high hardness, and fracture toughness [5]. However, there are challenges in fabrication of cemented WC. There is a high tendency of cracking during the fabrication of

cemented WC, which then limit use of other processing techniques. Fabrication of ceramics is impossible without using a binder. There are several binders that are used for cementing WC, this includes cobalt (Co), nickel (Ni) and iron (Fe). Co is regarded as a superior binder because it has good wetting behaviour with WC [5], however, Co is anticipated to cause human carcinogen [6].

There are numerous challenges with fabrication of cemented WC using additive manufacturing process (AM), including cracking and pore formation. Uhlmann et al, studied additive manufacturing of WC-Co, more pores were encountered when processing at low energy density [7]. Ku et al, also encountered porosity and cracking issue during the fabrication of cemented carbide using selective laser melting (SLM) process, the assumption was that these cracking were due to present of thermal stress while pores were assumed to be caused by poor powder flow. Using high binder content for cementation of WC yields segregation of cores areas that has large pool of binder with inhomogeneity distribution of WC particles [6]. The choice of binder for fabrication of WC is still an unresolved issue since these binders turns to wear rapidly leaving the WC grains unsupported [8]. The mechanical properties (hardness and toughness) of cemented WC depends on ratio of the WC and the binder, low content of binder with high content of WC yield high hardness and less toughness [4, 8]. Again, both hardness and toughness of cemented WC depends on grain size of WC, nanostructured material has higher hardness than coarser structure [4].

There are several techniques for production of MMCs , however, the choice of the process depends on the complexity of the component and the challenges encountered with process. Recent study shows laser cladding is a preferred process for refurbishment and coating purposes over traditional processes such as high velocity oxyfuel spraying, thermal plasma spray and submerged arc welding. Laser cladding has its special characteristics such as producing less dilution and low heat affected zone [9, 10, 11]. The common process for fabrication of material is via casting, however, this process requires post machining to final size, but since WC has very high melting and has high hardness, casting of WC is not favourable [12]. Another process attempted for fabrication of WC was to use a powder sintering process, however, this process has limitation in fabricating complex shapes [12]. Since laser cladding is preferred over other traditional process, Kim et al, has attempted to use direct energy deposition for fabrication of about 10mm X 86mm rectangular rod of WC-12Co varying energy density, more pores were observed on samples produced at low energy of  $4.1 \times 10^2 \text{ J/mm}^3$ . After performing compressive tests, transgranular cracks and intergranular were observed on samples that contained lots of porosity. AM process such as SLM has high tendency of producing porous components, however, formation of pores is minimized when reducing the laser scanning speed and hatch spacing [7]. In this study, laser cladding technique was used to produce WC-Ni coating by varying both WC and Ni content at fixed laser power and fixed laser scanning speed. Laser process parameter optimisation were done at fixed WC-Ni feed rate, fixed laser scanning speed while varying laser power. The effect of binder content and laser power were studied focusing on WC particles distribution, wear resistance and hardness.

## **2 Research methodology**

### **2.1 Materials**

This study used as-received mixture of non-spherical and spherical 32C WC powder and pure Ni(99.7Ni) to fabricate a 5mm thick coating on top of a 100 X 40 X 12mm mild steel plate. Both powders had particle size ranging from  $45\mu\text{m}$  - $90\mu\text{m}$ , WC powder was supplied by Weartech (Pty) LTD while pure nickel powder was supplied by TLS (Pty) LTD.

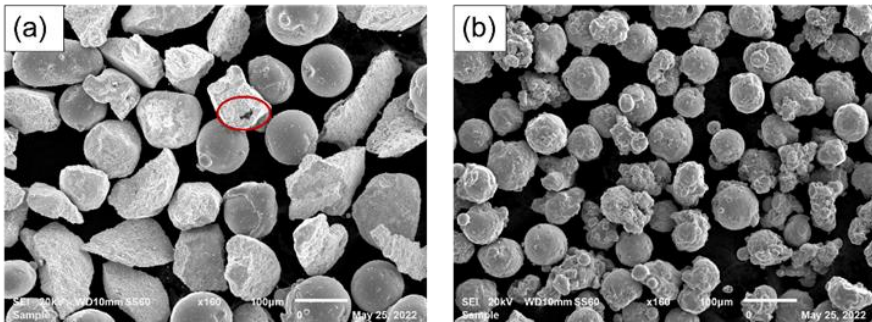


**Fig. 1.** SEM images showing morphologies of the powders, (a) WC, (b) Ni.

The morphology of the WC powder showed in Figure 1(a) as a mixture of both spherical and non-spherical. The non-spherical particles have pores circled in red, porous powder are likely to entrap oxygen which might lead to formation of pores during solidification of the melt.

## 2.2 Experimental procedure

Good metallurgical coating of WC-Ni deposited on a 100mm x 50mm x 12mm mild steel plate was achieved by using a laser cladding technique. An IPG laser that uses 1073 nm wavelength, 150 mm collimator, 200 µm fibre core and 300 mm lens was used to melt a stream of WC-Ni powder particles to produce a crack free intermittent coating of about 30 x 30 x 8mm (Figure 2) bonded onto the mild-steel substrate plate.



**Fig. 2.** WC-Ni coatings produced using cladding process.

Prior fabrication of a coating, the laser parameters were optimized. Then optimum laser parameters were developed by producing 90%WC-10%Ni clad using laser power of 1300W, 1500W, 1700W and 1900W at fixed laser scanning speed of 0.5m/min, while the powder flow fixed at Ni=0.2rpm and WC=1.8rpm, laser beam diameter fixed at 2mm, while argon used as shielding fixed at 15l/min and carrier gas fixed at 2l/min.

Selection of optimum laser process parameters were done by characterizing the samples using optical microscope and SEM. Selection of optimum laser parameters were based on obtaining less defect coating, full melting of Ni powder and good metallurgical bond to the

substrate. After selection of optimum parameters, two different mixtures of WC-Ni were studied by fabricating coatings at optimum laser parameters as shown in Table 1.

**Table 1.** Laser processing parameters for WC-Ni coating.

In-situ powder mixture	Laser power (W)	Scanning speed (m/min)	Powder feed rate (rpm)
70%WC-30%Ni	1300	0.5	1.4 WC, 0.6 Ni
90%WC-10%Ni	1300	0.5	1.8 WC, 0.2 Ni

Prior to the deposition, the base plates were sandblasted to remove possible scaling and contamination. A pure nickel butter layer was first deposited on the base with an aim of improving metallurgical bonding between the WC-Ni coating and the base, also to act as a barrier in preventing diffusion of elements from the steel base to the coating. WC-Ni coating of about sixteen laser clads tracks were produced at 60% overlap with the clad started from end-to-end.

### 2.3 Metallographic preparation and material characterization

Metallographic samples were machined from clads across the laser scanning direction using a cutting machine. The machined pieces were then mounted and ground with SiC grinding paper using water as a cooling medium. Grinding grit paper from 240, 320, 600, 800 to 1200 grit size were sequentially used.

After grinding, the samples were polished on Struers TegraForce-5 auto/manual polisher to a mirror finish surface of 0.04  $\mu\text{m}$  using the Med-Chem polishing cloth and diamond suspension liquid ranging from 9  $\mu\text{m}$ , 6  $\mu\text{m}$ , 3  $\mu\text{m}$  and 0.04  $\mu\text{m}$ . Samples were characterised in an unetched state using Olympus BX51M Optical Microscope (OM) and Jeol JSM 6510 SEM with energy dispersive spectroscopy (EDS).

### 2.4 Mechanical testing

In this study, two mechanical tests were performed on the clads: hardness and wear test. The hardness was done to determine the brittleness of the coating and the strength of the coating while wear test was done to determine the wear behaviour of the coating. The hardness measurement of the clads were measured using Matsuzawa Seiko micro-hardness Vickers model MHT-1 micro, the indentations were taken from the top of the coating through the nickel butter layer, through the heat affect zone and up to unaffected substrate. Tests were performed using a 500g load, the spacing between indentations was set at 600 $\mu\text{m}$ , and the dwell time of 10 s was applied.

The abrasive wear tests were performed according to ASTM G65 standard [13]. A 5kg load was used to push the sample against the rotating rubber lined wheel rotating at 200rpm, the sand was fed between the sample and the rotating wheel as shown in Figure 3. The abrasive quartz sand was used with a mixture of particle size ranging from 0.2-0.25mm. The wear tests were performed in intervals, in each interval the samples were weighed, the first interval was performed for 6.6 min to allow removal of unevenness, and the other 5 interval were performed for 13.2 min intervals.

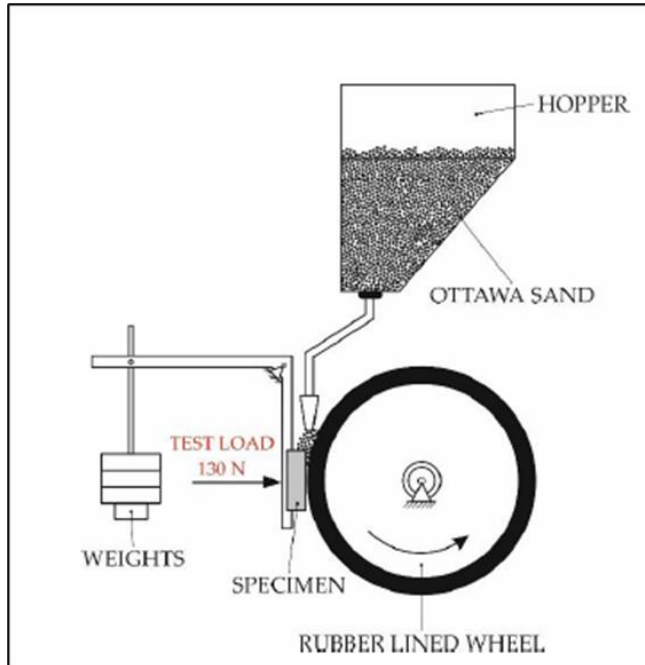


**Fig. 3.** G65 abrasive wear test [13]

## 3 Results and discussions

### 3.1 Optical microscope (OM) results analysis of WC-Ni coating

Figure 4 shows optical micrographs of WC-Ni coating, a crack free coating was achieved at low laser power of 1300W, however, more pores were observed at laser power of 1500W, 1700W and 1900W as compared to 1300W. Porosity formed at high heat input are likely due to evaporation effects [14], evaporation of low melted alloy which in this case is Ni, might cause deviation on chemical composition of the coating. Moreover, high heat input leads to entrapment of gas which causes pores as material solidifies.

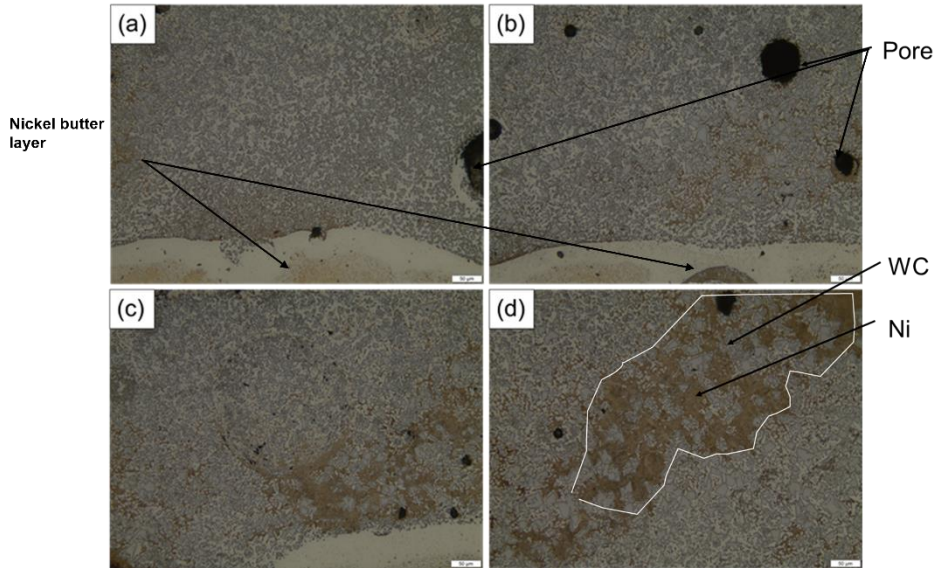


**Fig. 4.** Optical micrographs of 90%WC-10%Ni clads produced at fixed speed of 0.5m/min and different laser powers, (a) 1300W, (b) 1500W, (c) 1700W and (d) 1900W.

Optical micrographs shown in Figure 4(c) and (d) shows inhomogeneity distribution of WC particles in the matrix, this inhomogeneity distribution of WC lies just above the interphase forming an island as shown in a circled area in Figure 4(d). This inhomogeneity could be as a result of high heat input. The high heat input laser parameters yield high dilution, since the base were buttered with pure nickel, more Ni is expected to diffuse from the base buttered layer to the clads with increase in high heat input, therefore, binder content of the clad near the interphase increases which yield scattered packing of WC. This inhomogeneity and less packing of WC particle might yield lower hardness and less wear resistance because of more binder content [4, 8].

### 3.2 SEM results analysis of WC-Ni coating

Figure 5 present the SEM results of 90%WC-10Ni coating as produced from varying different laser power at fixed laser scanning speed.

SEM results in Figure 5(a) shows a closed packing of WC particles bonded with nickel, however, as laser power increased, inhomogeneity areas and islands were formed. There were also micro cracks examined on sample produced at high laser power as seen in sample (d). Prescence of micro cracks in a component can lead to delamination and spalling of the coating during impact loading [4].

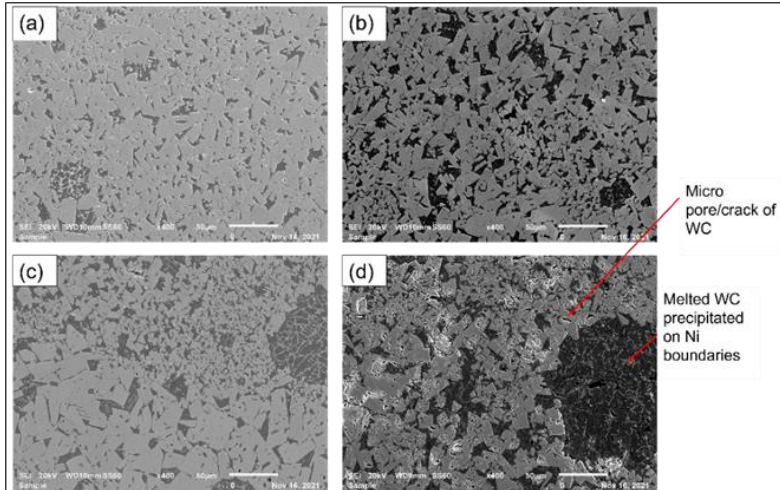


**Fig. 5.** Optical micrographs of 90%WC-10%Ni clads produced at fixed speed of 0.5m/min and different laser powers, (a) 1300W, (b) 1500W, (c) 1700W and (d) 1900W.

The SEM micrograph in Figure 6, shows a zoomed black area on sample produced at 1900W, this black like area has a columnar structure which might be due to high heat input causing partial melting of finer WC and diffusion of base plate element to the clad causing to segregations.

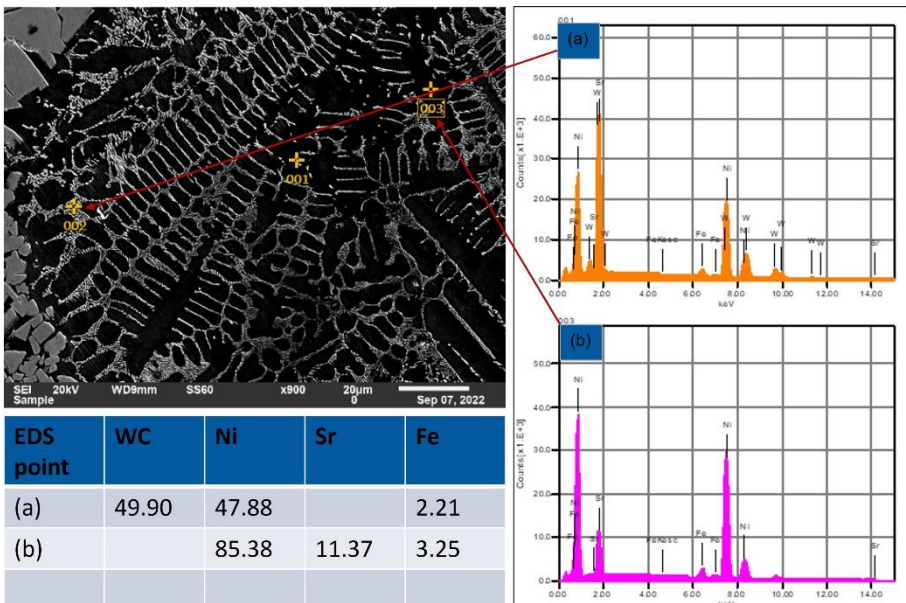


**Fig. 6.** SEM micrographs and EDS analysis of a 90%WC-10%Ni produced at 1900W showing a zoomed columnar structure.

EDS results in Figure 6(a) and (b) confirm the black background as Ni matrix while the columnar structure confirmed to contain both the WC and Ni. EDS also picked some percentage iron (Fe) and strontium (Sr) which might come from the mild steel base plate because of high dilution caused by high heat input.

When comparing WC-Ni micrographs for 90%WC and 70%WC produced at similar laser power of 1300W and 0.5m/min laser scanning speed as shown in Figure 7(a) and (b), sample(b) shows dense packing of WC particles as compared to sample(a), again, sample (b) has less cored area as compared to sample(a)

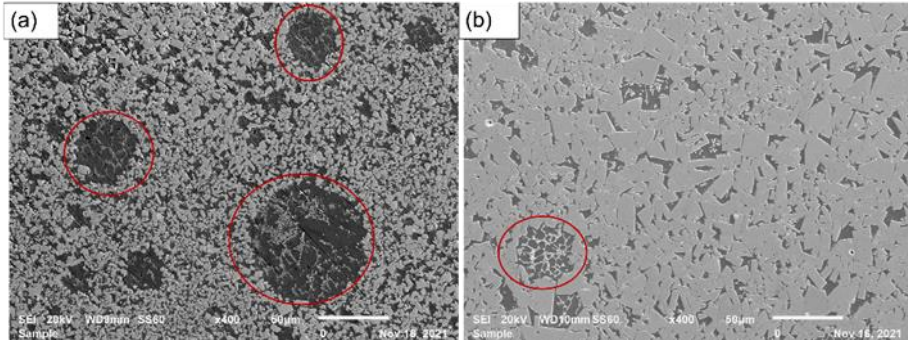


**Fig. 7.** SEM micrographs of WC-Ni clads, (a) 70wt% WC-30wt%Ni and (b) 90wt% WC – 10wt%Ni both produced at 1300W.

These cored like area as shown in Figure 7 circled in red, they are more like pore, however, they are not gas pore, when they are zoomed as shown in Figure 6, they contain a columnar structure of WC-Ni on a Ni matrix, they were observed near the interphase and mostly on 70tw% WC-30wt%Ni and on sample produced at high laser power.

### 3.3 Hardness results of WC-Ni coatings

Figure 8 present the hardness results of 90%WC-10%Ni and 70%WC-30%Ni coating as produced with similar laser power of 1300W and laser scanning speed of 0.5m/min. The 90%WC-10Ni sample shows high hardness as compared to 70%WC-30%Ni. This is because, the structure has dense packing of WC particle than 70%WC-30%Ni, moreover, 70%WC-30%Ni has more binder than 90%WC-10%Ni which makes it softer.

Both samples showed increase in hardness from butter layer area moving to the top of the clad, this is supported by observation analysis in figure 4 where less dense packing of WC particles were observed near the interphase as compared to the top of the clad. High binder content than WC yield lower hardness [4, 8].

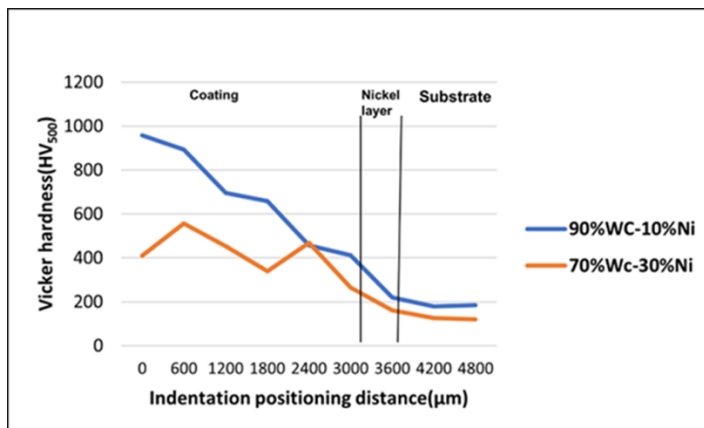


**Fig. 8.** Hardness results of 90% WC-10%Ni versus 70% WC-30%Ni.



### 3.4 Wear test results of WC-Ni coating

Figure 9 present wear results in weight loss versus time graph of 90%WC-10%Ni and 70%WC-30%Ni sample, both these WC-Ni coating were produced at fixed laser power of 1300W and fixed laser scanning speed of 0.5m/min.

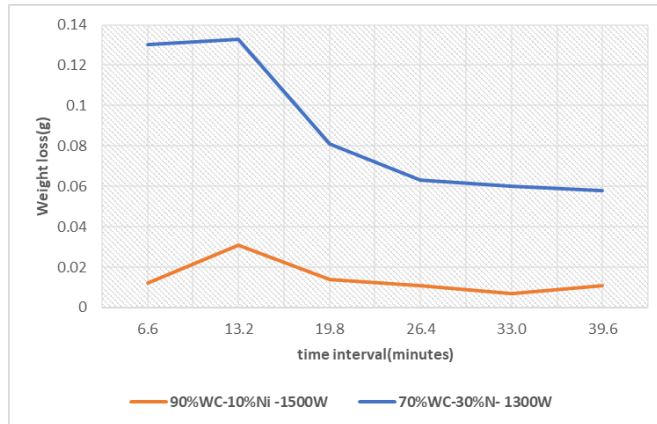


**Fig. 9.** Abrasive wear results of WC-Ni coating.

The 90%WC-10%Ni coating had lower weight loss as compared to 70%WC-30%Ni, this is presumably because of high WC content which causes higher hardness. Increasing the binder, decreases both hardness and wear as shown by 70%WC-30%Ni.

## 4 Conclusion

The study used a laser cladding technique in depositing WC-Ni coating on a mild steel base plate. Microstructure and mechanical properties (hardness and wear) of the coating were studied using OM, SEM, a wear tester, and a Vickers hardness tester.

- A crack free coating of 90%WC-10%Ni were successfully produced at lower laser power of 1300W and scanning speed of 0.5m/min using 2mm laser beam diameter; however.,
- Pores were observed on samples produced at higher laser power.
- Both hardness and wear resistance increased with increase in WC from 70%WC to 90%WC, however, 90%WC-10%Ni showed superior wear resistance than 70%WC-30%Ni, this was attributed to the uniform distribution of hard WC particles embedded on mild steel base that is buttered with nickel layer
- The micrographs for sample produced at higher laser power showed more inhomogeneity or rather scattered WC particle near the interphase, less dense packing of WC particle yield low hardness and low wear resistance.
- The micrographs for sample produced at higher laser power showed some segregated areas and pores, the segregated areas have columnar structure of WC-Ni. Future tests will include compression test to study the internal integrity, mainly focusing on WC inhomogeneity

## Acknowledgement

The authors like to thank manufacturing cluster within Council for Scientific and industrial Research for financial support and thank CSIR personnel who contributed to this work.

## References

1. M.R. Fishman, E. Rabkin, P. Levin, N. Frage, M. Dariel, A. Weisheit, R. Galun, B. Mordike, *Mater. Sci. Eng.* **302**, (2001)
2. E.T. Galvani, S. Simoes, C.N. Banoy, H. Rosa, *Ceram. Eng. Sci. Proc.* **17**, (2017)
3. J. Przybyłowics, J. Kusinski, *J. Mater. Proc. Tech.* **2**, (2001)
4. V. Bonache, M. Salvador, D. Busquests, P. Burguete, E. Martinez, F. Sapina, E. Sanchez, *Int. J. Refrac. Hard Met.* **29**, (2011)
5. N. Ku, J. Pittari, S. Kilczewski, A. Kudzal, *JOM.* **71**, (2019)
6. J. Pittari, H. Murdoch, S. Kilczewski, B. Hornbukle, J. Swab, K. Darling, J. Wright, *Int. J. Refrac. Hard Met.* **76**, (2018)
7. E. Uhlmann, G.W. Bergmann, *Proc. Cirp.* **15**, (2015)
8. I. Konyashin, F. Lachmann, B. Ries, A. Mazilkin, B. Straumal, C. Kubel, L. Lianes, B. Baretzky, *Scr. Mater.* **20**, (2014)
9. A.S. Reda, A. Hamid, A. Menam, I.S. Elden, E.H. Abdelrafea, S.H. Abdel, *Materials.* **16**, (2017)
10. K. Benarjy, Y. Kumar-Ravi, A. Jinoop, C. Paul, K. Bindra, *J. Mater. Sci. Perf.* **30**, (2021)
11. K. Van Acker, D. Vanhoywengen, R. Persoons, J. Vanggruderbeek, *Wear.* **258**, (2005)
12. K. Kim, G. Ham, S. Park, J. Cho, K. Lee, *Int. J. Refrac. Hard. Met.* **99**, (2021)
13. A. Czuprynski, *Materials.* **14**, (2021)
14. D. Hagedorn-Hansen, *Scholar.sun.ac.za* (2022)